

# The Bond Strength on Over Lapping Bars Using Pullout Test

*By Anis Rosyidah*

## The Bond Strength on Over Lapping Bars Using Pullout Test

Anis Rosyidah<sup>a,\*</sup>, J. Adhijoso Tjondro<sup>b</sup>, I Ketut Sucita<sup>a</sup>

<sup>a</sup> Civil Engineering Department, Politeknik Negeri Jakarta, Jl. Prof. GA. Siwabessy Kampus UI Depok, 16425, Indonesia

<sup>b</sup> Civil Engineering Department, Universitas Katolik Parahyangan Bandung, Indonesia

Corresponding author: \*anis.rosyidah@sipil.pnj.ac.id

**Abstract**— The behavior of reinforced concrete structures depends on sufficient bond strength between concrete and reinforcing steel. The perfect bond between the reinforcement surface and the concrete makes the transfer force work well. In this experiment, several forms of bars overlapped in the concrete and then tested pullout directly. This experiment is to get the tendency of the bond stress patterns that occur in overlapping bars. Another result of the study is the failure pattern of each specimen. The specimen size is 150×150×150 mm. In the center of the concrete cube is rib two overlapped bars. The reinforcement used plain and two ribs types of bars surface. The compression of concrete used is a minimum of 25 MPa. Furthermore, the specimen was subjected to a pullout test loaded in stages with 22 kN/minute speed. Loading stopped after the sample has collapsed. The pullout test uses the ASTM C234-91a standard. The failure pattern of plain reinforcement specimens with diameters of 12 mm, 16 mm, and 19 mm is a pullout or a slipped. The specimen with deform bar diameter 13 mm, 16 mm, and 19 mm occurs in splitting failure. The pullout test result, all samples in connection not yielded yet. The results show that the higher the bar diameter's development length, the higher the bond strength. The bond stress of the plain bar is smaller than the deform bar.

**Keywords**— Bond stress; slip; tension test; failure pattern; lap splice.

Manuscript received 30 May 2019; revised 24 Nov. 2020; accepted 24 Dec. 2020. Date of publication 30 Apr. 2021.  
IJASEIT is licensed under a Creative Commons Attribution-Share Alike 4.0 International License.



### 1. INTRODUCTION

The adequate bond strength between concrete and steel affects the performance of reinforced concrete structures. The force transfer can work well if there is a perfect bond between the reinforcing and concrete walls [1]. The formation of this good bond if the reinforcement's surface is coarse so that for structural reinforced concrete used deform bar. The reinforcement surface roughness is expressed in the bond index's relative area value [2]–[6].

Several previous research on the strength of reinforcing reinforcement at lap splice had been done [3], [7]–[15]. One of the results obtained with higher concrete quality and better aggregate quality and installed transverse reinforcement resulted in a better bonding reinforcement than without ties. Likewise, the deform and bar diameter's relative width has increased strength using transverse reinforcement [3]. Another study about lap spliced by Canbay and Frosh is two different collapse patterns: horizontal direction (side-splitting failure) and face-splitting failure. In splitting failure, the attached stress pattern's vertical direction tends to increase linearly [9], [16].

Study on the contribution of transversal reinforcement to the elongated joint with a headed [7] and bending of the hook reinforcement [13], the results obtained show that transverse reinforcement is effective in increasing the strength of anchoring on head reinforcement [5]. This result supports Darwin's research [8], with the transverse reinforcement installation, there is an additional strength of 25% [8]. To predict the strength of anchoring in the joint connection with the header bar, a very crucial component is the quality of the attachment and bearing strength, including the effect of transverse reinforcement, cover, and the distance of bar [7]. The bond strength of lap spliced based on parameters: bar diameter, development length, the compressive strength of concrete, and transversal reinforcement installed at the connection location have also been carried out [11], [14]. Research shows that transverse reinforcement contributes to the bond strength, especially in a large bar [11]; this result corresponds to ACI 318 [17].

In this study, the bond strength of lap spliced using the direct pullout with several deform reinforcing shapes. Previous studies have not explicitly revealed the contribution of bar deform shape to bar bond strength with concrete in lap spliced and the failure pattern, so this research needs action.

Determining the development length of reinforcement can use pullout testing directly with one bar, but a direct pullout test with double bars is necessary.

#### A. The Bond Mechanism

The bond stress is an interaction between reinforcement and surrounding concrete. Factors that influence this bond stress are complex. Three factors are determining the bond stress: adhesion, friction, and interlocking force. Reliable transfer of force between reinforcement and concrete is needed for optimal structural design. The mechanism of the force transfer from reinforcement to the surrounding concrete consists of (a) the adhesion between reinforcement with concrete, (b) friction force due to rough reinforcing surfaces, the shear force on the surface, and slip that occurs between steel bar with surrounding concrete, and (c) interlocking mechanism or bearing force on reinforcing form against concrete [9], [17]–[19]. The bond stress between reinforcement and concrete can be measured through a pullout test. The test results are analyzed and plotted in the bond stress and slip relationships graph, as presented in Figure 1 [20], [21].

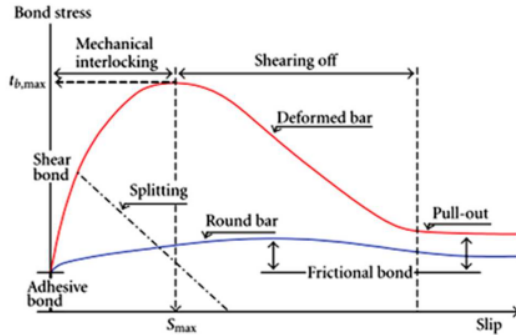


Fig. 1 The bond stress – slip relation [20], [21]

Fig. 1 illustrates the pattern of the relationship between the bond stress surrounding concrete and the slip that occurs. The adhesion value is the bond stress when the slip still zero. Friction is the maximum stress difference between the adhesion value [20]–[22]. Adhesion occurs when the load is still small on the deform bar, then friction and interlocking forces. If the concrete breaks, the graph has not reached the peak stress directly down, the failure pattern is brittle [22]. When the bond stress has reached the maximum, the pullout failure decreases and, at a certain point, tends to be constant then collapses [20], [21]. Several parameters that influence the mechanism of reinforcing bond stress with concrete are the bar rib's roughness and shape. The rib geometry contributes to bond strength.

The form and size of the reinforcing rib in some previous studies are realized in one parameter: the bond index or relative rib area ( $f_R$ ). Bond index is the ratio of high rib area to distance between ribs [31]–[23]. The bond index between 0.04 - 0.10 increases bond strength up to 40%. The interaction of bar rib with concrete reduces the risk of a split in the concrete [7], [23], [24]. The bond index formula ( $f_R$ ) is presented in the eq. 1.

$$f_R = \frac{d_o^2 - d_i^2}{4ds} \quad (1)$$

with  $f_R$  = bond index or relative rib area,  $d_o$  = outer diameter of rib reinforcement,  $d_i$  = inner diameter of rib reinforcement,  $d$  = nominal diameter of reinforcement,  $s$  = distance between rib as to as.

#### B. Bond Stress on a Lap Splice

The bond stress distribution in the lap splice is reading the strain during testing. The bond stress formula of the lap spliced ( $\tau_i$ ) is presented in the Eq. 2 [25], [26].

$$\tau_i = \frac{d_b E_s}{4} \left[ \frac{(\epsilon_i - \epsilon_{i-1})}{(x_i - x_{i-1})} \right] \quad (2)$$

with  $d_b$  = bar diameter,  $E_s$  = elasticity modulus of steel,  $\epsilon_i$  = axial strain,  $x_i$  = strain gauge position (mm).

The value of bond strength in the lap spliced can know with the assumption that the strain that occurs in the free end is zero. The stress that occurs in the short and long lap spliced is a different; the stress value along short lap spliced tends to be the same. The bond stress of each bar at the lap spliced, the most significant number occurs on the side of the reinforcement pulled, then the smaller the middle and equal to zero at the free end [6], [25], [27].

## II. THE MATERIAL AND METHOD

The specimens were cube concrete with a dimension of 150 mm × 150 mm × 150 mm, in the middle installed two overlapping bars (Fig. 2). Concrete compressive strength ( $f_c$ ) is 29 MPa. The deform bars consists of fishbone rib (ST) brand TGS (Toyogiri Iron Steel) and slop rib (SC) Brand KS (Krakatau Steel) with diameters D13 mm, D16 mm, and D19 mm (Fig. 3). The results of the two types of rib were compared with the bond strength of the plain bar.

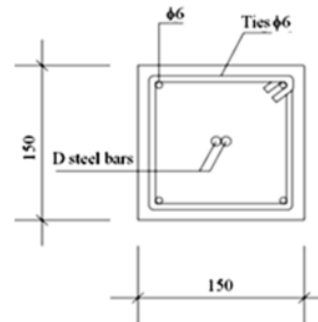


Fig. 2 Specimen dimensions

Pullout testing uses a Universal Testing Machine (UTM). The specimens located in the middle with both ends of the bars clamped (Fig. 4). The sample tested after the specimen is more than 28 days old. After 28 days passed, the sample tested direct pullout. A strain gauge installed on one of the bars to determine the bond stress on the other overlapping reinforcement, as shown in Fig. 5 [25]. A strain gauge installed on one of the bars determines the bond stress on the additional overlapping bar, as shown in Figure 4 [22]. The strain gauge outputs analyzed using Eq. (2) to get bond stress and the pattern of failure that occurs from each specimen.

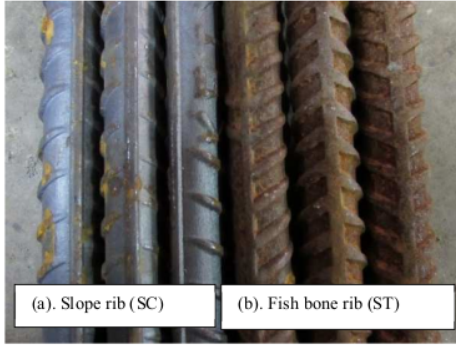


Fig. 3 Deform bars (a). slope rib (SC), (b). fishbone rib (ST)



Fig. 4 The setting of pullout testing using UTM

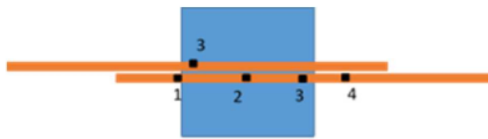


Fig. 5 Strain gauge placement layout

### III. RESULTS AND DISCUSSION

TABLE I  
THE VALUE OF RELATIVE RIB AREA (BOND INDEX)

| Form of rib bars   | D   | n     | Rib area $A_r$ (mm <sup>2</sup> ) | Rib spacing $L_d$ (mm) | Rib angle ( $^\circ$ ) | bond index $f_r$ | Average $f_r$ |
|--------------------|-----|-------|-----------------------------------|------------------------|------------------------|------------------|---------------|
| Slope rib (SC)     | D13 | 1     | 60.575                            | 8                      | 65                     | 0.1094           | <b>0.11</b>   |
|                    |     | 2     | 62.468                            | 8                      | 65                     | 0.1145           |               |
|                    |     | 3     | 56.789                            | 8                      | 65                     | 0.0965           |               |
|                    | D16 | 1     | 97.014                            | 10                     | 65                     | 0.1089           | <b>0.13</b>   |
|                    |     | 2     | 106.479                           | 10                     | 65                     | 0.1312           |               |
|                    |     | 3     | 108.845                           | 10                     | 65                     | 0.1368           |               |
| Fish bone rib (ST) | D13 | 1     | 144.812                           | 12                     | 65                     | 0.1119           | <b>0.11</b>   |
|                    |     | 2     | 136.293                           | 12                     | 65                     | 0.0977           |               |
|                    |     | 3     | 141.972                           | 12                     | 65                     | 0.1067           |               |
|                    | D16 | 1     | 37.2                              | 6                      | 60                     | 0.1753           | <b>0.16</b>   |
|                    |     | 2     | 30.0                              | 6                      | 60                     | 0.1271           |               |
|                    |     | 3     | 37.2                              | 6                      | 60                     | 0.1753           |               |
| D19                | 1   | 68.8  | 8                                 | 60                     | 0.1481                 | <b>0.14</b>      |               |
|                    | 2   | 68.8  | 8                                 | 60                     | 0.1481                 |                  |               |
|                    | 3   | 64.0  | 8                                 | 60                     | 0.1276                 |                  |               |
| D19                | 1   | 122.0 | 10                                | 60                     | 0.1599                 | <b>0.15</b>      |               |
|                    | 2   | 120.0 | 10                                | 60                     | 0.1544                 |                  |               |
|                    | 3   | 118.0 | 10                                | 60                     | 0.1489                 |                  |               |

The rib bar measurement to get bond index or relative rib area is shown in Table 1. The slope rib bar threads' bond index values ranged from 0.11 to 0.13, while the fishbone rib bars were obtained from 0.14 to 0.16. The bond index on the slope rib bars is lower than the reinforcement of the fishbone rib.

#### A. The Failure Pattern of Specimen

The collapse in the specimen of the mutual connection of plain reinforcement in diameter 12 mm, 16 mm, and 19 mm is a pullout or a reinforced bar; in Figure 5, there is no visually showing splitting. The plain bars specimen of the diameter: 12 mm, 16 mm, and 19 mm undergo pullout failure, Fig. 6 there is no showing splitting.

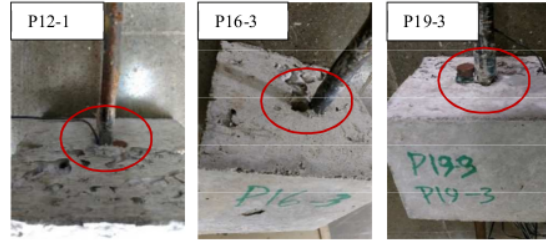


Fig. 6 The pullout failure pattern of plain bars specimen

In contrast to plain bars, damage of the slope rib bars the diameter of 13 mm, 16 mm, and 19 mm is splitting failure (Fig. 7).



Fig. 7 The splitting failure pattern of slope rib bars specimen (SC)

All the specimen of the fishbone rib failure is splitting (Fig. 8).



Fig. 8 The splitting failure pattern of fishbone rib bars specimen (ST)

The damage pattern of the two rib types shows the splitting failure. In Fig. 7 and 8, cracks starting from around the bars radiate to the concrete's outer side. The small diameter (D13) of the two rib types specimen is crack, but bigger than D13 the concrete is a break, even though the sample was put in the stirrup. This pattern of failure is similar to the research from Gaurav (2017), Canbay (2005), Lagier (2016), and Gangolu (2016). The influence of rib causes an interlocking mechanism, where the force of concrete distributed through

the rib of the bar. As a result of distribution the longitudinal and radial directional forces so that the concrete presses occur, if the stress arises beyond the concrete compressive capacity, it will cause a radial crack, and it continues to develop, it causes splitting failure [9], [26], [28]–[30]. In the plain bars, Fig. 6 shows the bar has slipped in the plain bars, there is no crack on the concrete surface. This failure pattern is identical with M. N. Hassan's (2012) research that the lap spliced of plain reinforcement has failed due to the bond between reinforcement and concrete to slip [31].

### B. The Bar Stress and the Bond Stress on Lap Splice

Experimental results of the lap splice showed none of the bars undergo yield. In Table 2 and Fig. 9, there are not  $f_s/f_y$  ratio greater than or equal to 1. The most effective rate is 0.97 (SC13\_3). The higher the diameter of the reinforcement, the lower the stress. The plain bar stress is smaller than a deform bar.

TABLE II  
THE EXPERIMENT RESULT AND THE FAILURE OF SPECIMEN

| No | Specimen | Dia. bar (mm) | L <sub>d</sub> /d | P <sub>max</sub> (N) | f <sub>s</sub> (MPa) | f <sub>y</sub> (MPa) | f <sub>b average</sub> (MPa) | f <sub>s</sub> /f <sub>y</sub> | Failure Pattern |
|----|----------|---------------|-------------------|----------------------|----------------------|----------------------|------------------------------|--------------------------------|-----------------|
| 1  | P13_1    | 11.84         | 12.67             | 11040                | 100                  | 338                  | 1.98                         | 0.30                           | Pullout         |
| 2  | P13_2    | 11.84         | 12.67             | 15265                | 139                  | 338                  | 2.74                         | 0.41                           | Pullout         |
| 3  | P13_3    | 11.84         | 12.67             | 8916                 | 81                   | 338                  | 1.60                         | 0.24                           | Pullout         |
| 4  | SC13_1   | 12.87         | 11.66             | 39208                | 302                  | 347                  | 6.47                         | 0.87                           | Splitting       |
| 5  | SC13_2   | 12.87         | 11.66             | 36084                | 278                  | 347                  | 5.95                         | 0.80                           | Splitting       |
| 6  | SC13_3   | 12.87         | 11.66             | 43954                | 338                  | 347                  | 7.25                         | 0.97                           | Splitting       |
| 7  | ST13_1   | 13.03         | 11.52             | 47521                | 357                  | 442                  | 7.74                         | 0.81                           | Splitting       |
| 8  | ST13_2   | 13.03         | 11.52             | 45661                | 343                  | 442                  | 7.44                         | 0.78                           | Splitting       |
| 9  | ST13_3   | 13.03         | 11.52             | 45886                | 344                  | 442                  | 7.48                         | 0.78                           | Splitting       |
| 10 | P16_1    | 15.96         | 9.40              | 10757                | 54                   | 318                  | 1.43                         | 0.17                           | Pullout         |
| 11 | P16_2    | 15.96         | 9.40              | 17092                | 85                   | 318                  | 2.27                         | 0.27                           | Pullout         |
| 12 | P16_3    | 15.96         | 9.40              | 13474                | 67                   | 318                  | 1.79                         | 0.21                           | Pullout         |
| 13 | SC16_1   | 15.96         | 9.40              | 42382                | 212                  | 341                  | 5.64                         | 0.62                           | Splitting       |
| 14 | SC16_2   | 15.96         | 9.40              | 47968                | 240                  | 341                  | 6.38                         | 0.70                           | Splitting       |
| 15 | SC16_3   | 15.96         | 9.40              | 28912                | 145                  | 341                  | 3.85                         | 0.42                           | Splitting       |
| 16 | ST16_1   | 15.87         | 9.45              | 47973                | 243                  | 450                  | 6.42                         | 0.54                           | Splitting       |
| 17 | ST16_2   | 15.87         | 9.45              | 44475                | 225                  | 450                  | 5.95                         | 0.50                           | Splitting       |
| 18 | ST16_3   | 15.87         | 9.45              | 39015                | 197                  | 450                  | 5.22                         | 0.44                           | Splitting       |
| 19 | P19_1    | 19.04         | 7.88              | 17677                | 62                   | 283                  | 1.97                         | 0.22                           | Pullout         |
| 20 | P19_2    | 19.04         | 7.88              | 3340                 | 12                   | 283                  | 0.37                         | 0.04                           | Pullout         |
| 21 | P19_3    | 19.04         | 7.88              | 20040                | 70                   | 283                  | 2.24                         | 0.25                           | Pullout         |
| 22 | SC19_1   | 18.89         | 7.94              | 31366                | 112                  | 380                  | 3.53                         | 0.30                           | Splitting       |
| 24 | SC19_3   | 18.89         | 7.94              | 37600                | 134                  | 380                  | 4.23                         | 0.35                           | Splitting       |
| 25 | ST19_1   | 19.03         | 7.88              | 44265                | 156                  | 420                  | 4.94                         | 0.37                           | Splitting       |
| 26 | ST19_3   | 19.03         | 7.88              | 47214                | 166                  | 420                  | 5.27                         | 0.40                           | Splitting       |

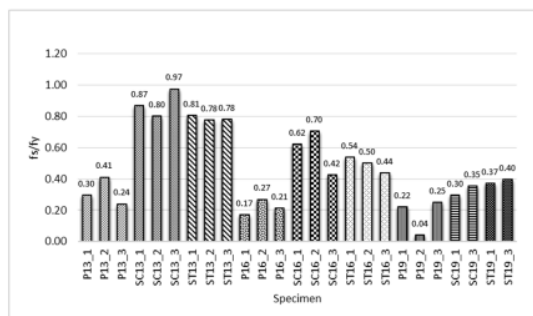


Fig. 9 The bar stress to yield stress ratio of each specimen

The results also show that the higher the ratio of the length of the lap splice (L<sub>d</sub>) to the bar diameter (d) the more significant the stress that occurs in the bar (Fig. 10). The trend of this result is in equal with some previous experiments [3], [9], [27], [29].

Based on Fig. 10, the plain bar has a lower reinforcement stress value than the deform reinforcement, the smaller L<sub>d</sub> / d ratio also shows a decrease in stress. With the same L<sub>d</sub>/d ratio, the reinforcement stress of fishbone rib tends to be higher than the slope rib.

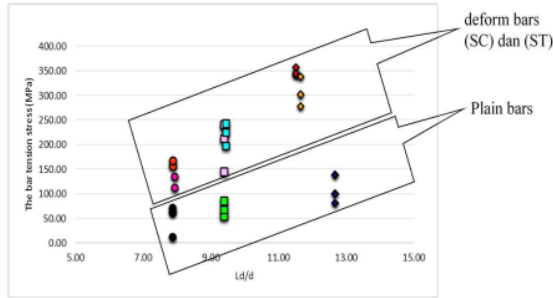


Fig. 10 The stress bar vs the lap spliced to bar diameter

Likewise, with the average bond stress on reinforcement ( $f_b$ ), the plain bar is lower than a deform bar. From Figure 11, the average bond stress of the fishbone rib is higher than the slope rib.

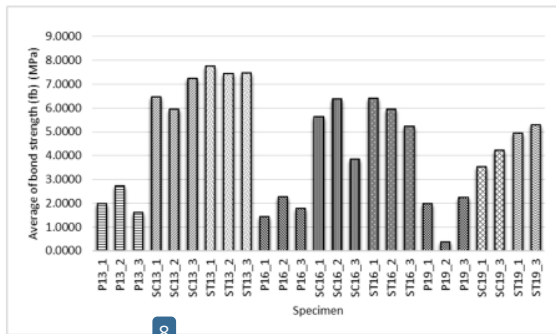


Fig. 11 The average bond stress of specimen

With the same lap splice length and the bar diameter increases, the decreasing stress value is obtained.

The slope rib and fishbone rib have different rib angles, the spacing of rib, and rib height, so the bond index is desperate. The fishbone rib has a higher bond index than the slope rib, so the bond strength is also high. This result is by previous research from Bosco and Silva that the higher the bond index value, the higher the bond strength of the reinforcement [29], [32], [33]. In Silva's research and the bond index, the rib angle is very influential on bond strength. The smaller the rib angle results in, the higher the ultimate bond strength. In this case, the edge of the fishbone rib was lower than the slope rib; it turned out that the average bond stress of fish bones ribs to be more significant than the slope rib.

### C. The Bond Stress Distribution in Lap Splice

Bond stress distribution between the concrete reinforcement at the lap splice presented with locations strain gauge in Fig. 12.

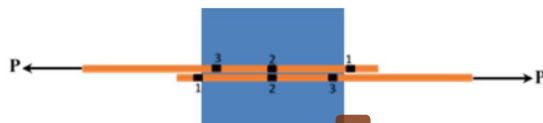


Fig. 12 The measurement point of bond stress

Determination bond stress distribution between steel bar with concrete on the lap splice based on the strain gauge output is attached to the reinforcement (Fig. 12) point no. 2 and 3. For point no. 1 at the free end, the furthest side of the reinforcement position, assuming the value is zero [34-27 ang, 2017). This stress distribution uses eq. 2. The graph of stress distribution is plotted based on the percentage of the maximum tensile axial forces that can resist during testing pullout, starting at 15%, 25%, 50%, 75%, and 100% of  $P_{max}$ . The bond stress distribution of lap splice D13 presented in Fig. 13, 14, and 15.

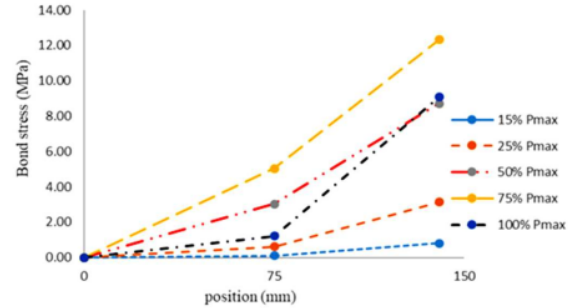


Fig. 13 Bond stress distribution based on position with specific axial force on P13 specimen

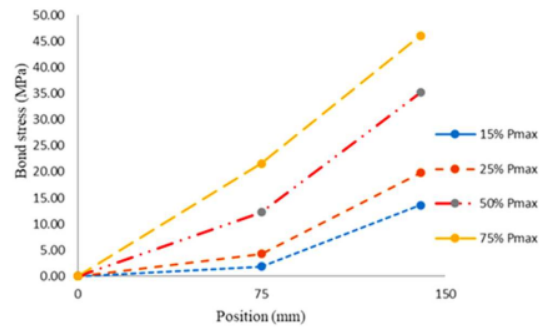


Fig. 14 Bond stress distribution based on position with specific axial force on SC13 specimen

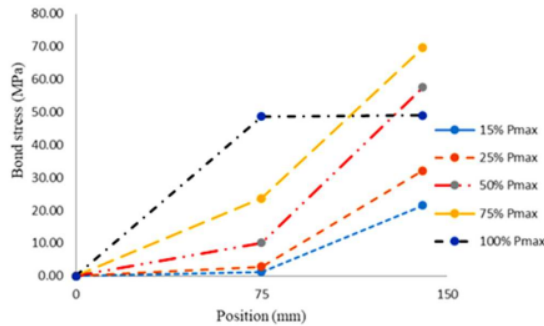


Fig. 15 Bond stress distribution based on position with specific axial force on ST13 specimens

The pattern of bond stress distribution on specimens P13, SC13, and ST13 shows the same forms. However, ST13 samples with stress at 100% of maximum loading at points 2 & 3 obtained relatively equal value, whereas the other stress distributions point 2 tend to be smaller than point 3. The bond stress distribution of the lap splice of steel bar with D16 shown in Fig. 16, 17, and 18.

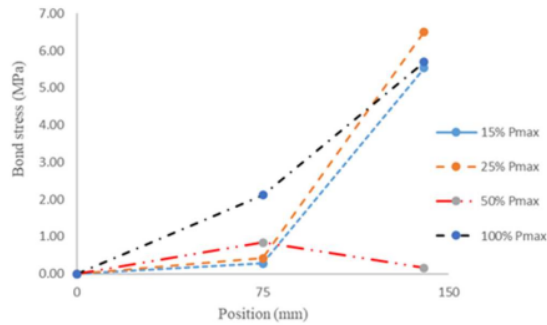


Fig. 16 Bond stress distribution based on position with specific axial force on P16 specimen

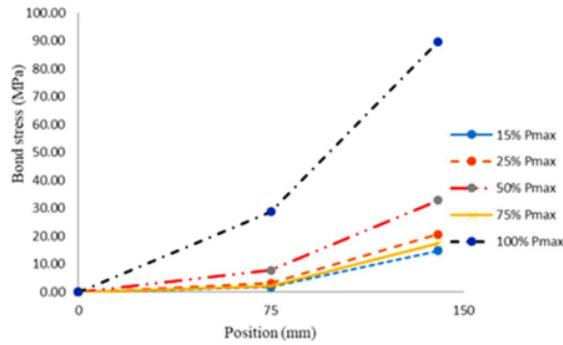


Fig. 17 Bond stress distribution based on position with specific axial force on SC16 specimen

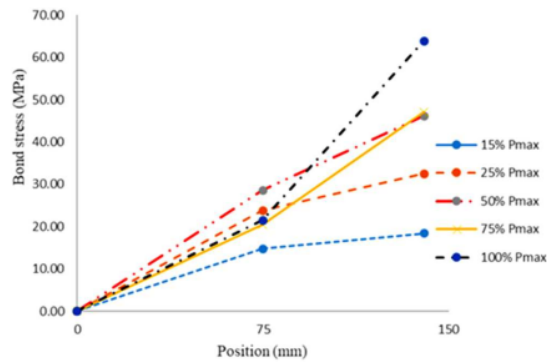


Fig. 18 Bond stress distribution based on position with specific axial force on ST16 specimen

The bond stress distribution in specimens P16, SC16, and ST16, have a relatively similar pattern, except for specimen P16, when the load is 50% of maximum loading, the stress value at point 2 is more significant than at point 3.

Furthermore, the bond stress distribution of lap splice of steel bar with D19 is shown in Fig. 19, 20, and 21.

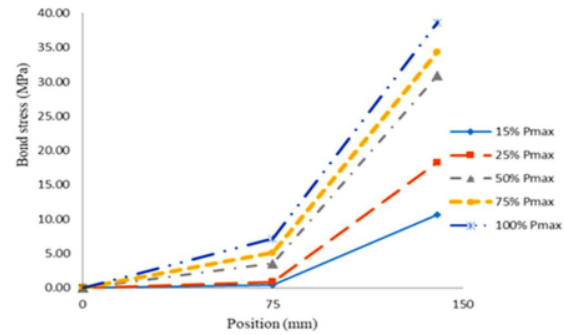


Fig. 19 Bond stress distribution based on position with specific axial force on P19 specimen

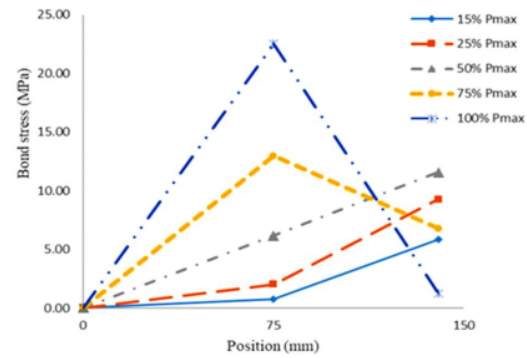


Fig. 20 Bond stress distribution based on position with specific axial force on SC19 specimen

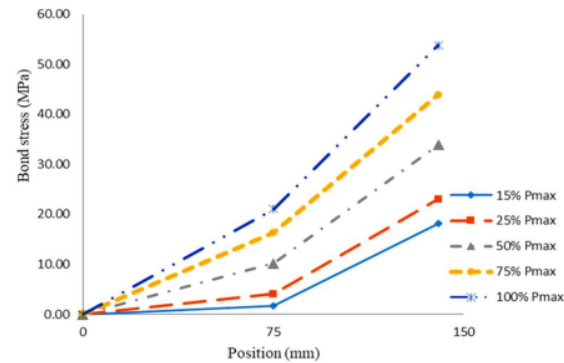


Fig. 21 Bond stress distribution based on position with specific axial force on ST19 specimen

The pattern of bond stress distribution at specimens of P19 and ST19 shows the same forms while SC19 samples with 75% and 100% of maximum loading at point 2, the values obtained are higher than point 3, whereas other stress distributions at point 2 tend to be smaller than point 3.

The bond stress distribution of lap splice of experimental results taken from 3 points, no. 1 is the point-free end with

value 0 and position 0. Point no. 2 is located in the center of reinforced concrete in concrete, a distance of 75 mm from the outer side. Point no. 3 is at a distance of 140 mm from position 0. The stress distribution pattern of all specimens tends to be similar in plain bars, threads, and different reinforcing diameters. These results have the same shape as the results of previous studies by Bournas (2011) and Lagier (2016) [35], [36].

#### IV. CONCLUSION

Based on the experiment of all specimens can be concluded as follows. Pattern damage specimen's plain reinforcement diameter of 12 mm, 16 mm, and 19 mm are pullout failures. The reinforced of both slope rib and fishbone rib, diameter 13 mm, 16 mm, and 19 mm undergo splitting collapse. The pullout lap splices all specimens have not the yield bar yet. There is only one specimen with a ratio of  $f_s / f_y$  reaching 0.97, a specimen of 13 mm diameter of slope rib. The results show that the higher the ratio lap splice length ( $L_d$ ) to the bar diameter, the higher the average bond stress obtained. The bond stress of the plain bar is smaller than the deform bar. The experiment results show that the higher the length of the development length ( $L_d$ ) to the reinforcement diameter, the higher the average bond stress obtained. In bond stress of plain bar that occurs is smaller than the bar of a slope rib screw and fishbone rib.

#### NOMENCLATURE

|              |                                     |     |
|--------------|-------------------------------------|-----|
| $E_s$        | elasticity modulus of steel         | MPa |
| $d_e$        | outer diameter of rib reinforcement | mm  |
| $d_i$        | inner diameter of rib reinforcement | mm  |
| $d$          | nominal diameter of reinforcement   | mm  |
| $f_R$        | bond index or relative rib area     |     |
| $s$          | distance between rib as to as       | mm  |
| $\epsilon_i$ | axial strain                        |     |
| $\tau$       | The bond stress of the lap spliced  | MPa |

#### ACKNOWLEDGMENT

We are grateful to P3M Politeknik Negeri Jakarta, Civil Engineering Department Universitas Katolik Parahyangan, and all parties who have helped this research.

#### REFERENCES

- [1] M. Dehestani and S. S. Mousavi, "Modified steel bar model incorporating bond-slip effects for embedded element method," *Constr. Build. Mater. J.*, vol. 81, no. April, pp. 284–290, 2015.
- [2] G. Metelli, J. Cairns, and G. Plizzari, "The influence of percentage of bars lapped on performance of splices," *Mater. Struct.*, pp. 2983–2996, 2014.
- [3] J. Zuo and D. Darwin, "Splice strength of conventional and high relative rib area bars in normal and high-strength concrete," *ACI Struct. J.*, vol. 97, no. 4, pp. 630–641, 2000.
- [4] D. Ertzibengoa, S. Matthys, and L. Taerwe, "Bond behaviour of flat stainless steel rebars in concrete," *Mater. Struct.*, vol. 45, no. 11, pp. 1639–1653, 2012.
- [5] A. Rosyidah, I. K. Sucita, and F. Hidayat, "The Bond Strength of Glass Fiber Reinforced Polymer ( GFRP ) Reinforcement with Monolith Concrete," *IJASEIT*, vol. 8, no. 2, pp. 495–500, 2018.
- [6] Q. Yu, J. Sun, Z. Xu, L. Li, Z. Zhang, and S. Yu, "Mechanical analysis of grouted sleeve lapping connector," *Appl. Sci.*, vol. 9, no. 22, Nov. 2019.
- [7] S.-C. Chun, "Lap Splice Tests Using High-Strength Headed Bars of 550 MPa (80 ksi) Yield Strength," *ACI Struct. J.*, vol. 112, no. 6, pp. 679–688, 2015.
- [8] D. Darwin, "Tension development length and lap splice design for reinforced concrete members," *Prog. Struct. Eng. Mater.*, vol. 7, no. 4, pp. 210–225, 2005.
- [9] E. Canbay and R. J. Frosch, "Bond strength of lap-spliced bars," *ACI Struct. J.*, vol. 102, no. 4, pp. 605–614, 2005.
- [10] E. Canbay and R. J. Frosch, "Design of lap-spliced bars: Is simplification possible?," *ACI Struct. J.*, vol. 103, no. 3, pp. 444–451, 2006.
- [11] T. K. Hassan, G. W. Lucier, and S. H. Rizkalla, "Splice strength of large diameter, high strength steel reinforcing bars," *Constr. Build. Mater.*, vol. 26, no. 1, pp. 216–225, 2012.
- [12] H. Hwang, "Local Bond Strength based Lap Splice Length Model of Reinforcing Bars," in *Advances in Civil, Structural and Mechanical Engineering*, 2015, pp. 25–29.
- [13] H. J. Hwang, H. G. Park, and W. J. Yi, "Development length of standard hooked bar based on non-uniform bond stress distribution," *ACI Struct. J.*, vol. 114, no. 6, pp. 1637–1648, 2017.
- [14] J. Yuan and B. Graybeal, "Bond of reinforcement in ultra-high-performance concrete," *ACI Struct. J.*, vol. 112, no. 6, pp. 851–860, 2015.
- [15] G. Gaurav and B. Singh, "Bond strength prediction of tension lap splice for deformed steel bars in recycled aggregate concrete," *Mater. Struct. Constr.*, vol. 50, no. 5, pp. 1–23, 2017.
- [16] H. J. Hwang, H. G. Park, and W. J. Yi, "Nonuniform bond stress distribution model for evaluation of bar development length," *ACI Struct. J.*, vol. 114, no. 4, pp. 839–849, 2017.
- [17] ACI Committee 408, "ACI 408R-03 Bond and Development of Straight Reinforcing Bars in Tension," in *American Concrete Institute*, 2003, pp. 1–49.
- [18] G. Xing, C. Zhou, T. Wu, and B. Liu, "Experimental study on bond behavior between Plain Reinforcing Bars and concrete," *Adv. Mater. Sci. Eng.*, vol. 18, no. 10, pp. 745–752, 2015.
- [19] X. Gao, N. Li, and X. Ren, "Analytic Solution for The Bond Stress-Slip Relationship Between Rebar and Concrete," *Constr. Build. Mater.*, vol. 197, pp. 385–397, 2019.
- [20] H. Shima, L. L. Chou, and H. Okamura, "Micro and macro models for bond in reinforced concrete," *Journal of the Faculty of Engineering, The University of Tokyo*, vol. XXXIX, no. 2, pp. 133–194, 1987.
- [21] S. Hong and S. K. Park, "Uniaxial bond stress-slip relationship of reinforcing bars in concrete," *Adv. Mater. Sci. Eng.*, vol. 2012, no. April, 2012.
- [22] M. Teresa, G. Barbosa, E. De Souza, and S. Filho, "Analysis of the Relative Rib Area of Reinforcing Bars Pull Out Tests 4 . Experimental Results and Discussion," *Mater. Res.*, vol. 11, no. 4, pp. 453–457, 2008.
- [23] G. Metelli and G. A. Plizzari, "Influence of the relative rib area on bond behaviour," *Mag. Concr. Res.*, vol. 66, no. 6, pp. 277–294, 2014.
- [24] Sung-Chul Chun; Sung-Ho Lee; and Bohwan Oh, "Compression Splices in Confined Concrete of 40 and 60 MPa (5800 and 5700 psi) Compressive Strengths," *ACI Struct. J.*, vol. 107, no. May-June, pp. 2010–2012, 2011.
- [25] D. A. Bournas and T. C. Triantafillou, "Bond Strength of Lap-Spliced Bars in Concrete Confined with Composite Jackets," *J. Compos. Constr.*, vol. 15, no. 2, pp. 156–167, 2011.
- [26] F. Lagier and J. Charron, "Behaviour of tension lap splice specimens in UHPRFC," in *9th RILEM International Symposium on Fiber Reinforced Concrete - BEFIB 2016; 19-21 September 2016, Vancouver, Canada*, 2016, no. October, pp. 75–89.
- [27] F. Lagier, B. Massicotte, and J. Charron, "Behaviour of Tension Lap Splice Specimens," in *9th RILEM International Symposium on Fiber Reinforced Concrete*, 2016, no. October, pp. 75–89.
- [28] G. Gaurav and B. Singh, "Bond strength prediction of tension lap splice for deformed steel bars in recycled aggregate concrete," *Mater. Struct. Constr.*, vol. 50, no. 10, 2017.
- [29] A. R. Gangolu, P. R. S., and E. Rolf, "Prediction of Analytical Bond Strength of Lap Splices in Tension," in *Proceedings of the 9th International Conference on Fracture Mechanics of Concrete and Concrete Structures*, 2016, no. June.
- [30] Q. Yu, X. Xu, W. Yuan, Z. Xu, and X. Lu, "Experimental Study of Mechanical Properties of Grouted Sleeve Lapping Connector with Different Lap Lengths under Tensile Load," *Hunan Daxue Xuebao/Journal Hunan Univ. Nat. Sci.*, vol. 44, no. 9, pp. 82–91, Sep. 2017.
- [31] M. N. Hassan and L. R. Feldman, "Behavior of Lap-Spliced plain steel bars," *ACI Struct. J.*, vol. 109, no. 2, pp. 235–244, 2012.
- [32] C. Bosco and F. Tondolo, "Bond Performance in Machined Reinforcing Bar for Reinforced Concrete," *Appl. Mech. Mater.*, vol.



- 166–169, pp. 828–831, 2012.
- [33] L. C. P. S. Filho, V. Silva, V. I. D. Bosco, L. E. S. Gomes, M. P. Barbosa, and M. S. Lorrain, “Analysis of the influence of rebar geometry variations on bonding strength in the pullout test,” in *Bond in Concrete 2012*, 2012, no. June, pp. 63–68.
- [34] C. W. Tang, “Uniaxial bond stress-slip behavior of reinforcing bars embedded in light weight aggregate concrete,” *Struct. Eng. Mech.*, vol. 62, no. 5, pp. 651–661, 2017.
- [35] D. A. Bournas, T. C. Triantafillou, and M. Asce, “Bond Strength of Lap-Spliced Bars in Concrete Confined with Composite Jackets,” no. April, pp. 156–168, 2011.
- [36] F. Lagier, B. Massicotte, and J. Charron, “Experimental investigation of bond stress distribution and bond strength in unconfined UHPFRC lap splices under direct tension,” *Cem. Concr. Compos.*, vol. 74, pp. 26–38, 2016.

# The Bond Strength on Over Lapping Bars Using Pullout Test

ORIGINALITY REPORT

11%

SIMILARITY INDEX

## PRIMARY SOURCES

- 1 [www.insightsociety.org](http://www.insightsociety.org) 27 words — 1%  
Internet
- 2 [orca.cf.ac.uk](http://orca.cf.ac.uk) 26 words — 1%  
Internet
- 3 "ACI Structural Journal September-October 2012 V. 109 No. 5 Complete", ACI Structural Journal, 2012 19 words — 1%  
Crossref
- 4 D. A. Bournas, T. C. Triantafillou. "Bond Strength of Lap-Spliced Bars in Concrete Confined with Composite Jackets", Journal of Composites for Construction, 2011 18 words — < 1%  
Crossref
- 5 Jun Zhao, Gaochuang Cai, Junmin Yang. "Bond-slip behavior and embedment length of reinforcement in high volume fly ash concrete", Materials and Structures, 2015 17 words — < 1%  
Crossref
- 6 [ascelibrary.org](http://ascelibrary.org) 16 words — < 1%  
Internet
- 7 "Compression Splices in High-Strength Concrete of 100 MPa (14,500 psi) and Less", ACI Structural Journal, 2011 15 words — < 1%  
Crossref

- 
- 8 Samanta Robuschi, Jakob Sumearll, Ignasi Fernandez, Karin Lundgren. "Bond of naturally corroded, plain reinforcing bars in concrete", Structure and Infrastructure Engineering, 2020  
Crossref 15 words — < 1%
- 
- 9 Kim Hung Mo, Phillip Visintin, U. Johnson Alengaram, Mohd Zamin Jumaat. "Bond stress-slip relationship of oil palm shell lightweight concrete", Engineering Structures, 2016  
Crossref 14 words — < 1%
- 
- 10 [civilejournal.org](http://civilejournal.org)  
Internet 14 words — < 1%
- 
- 11 [insightsociety.org](http://insightsociety.org)  
Internet 14 words — < 1%
- 
- 12 [www.i-asem.org](http://www.i-asem.org)  
Internet 13 words — < 1%
- 
- 13 "High Tech Concrete: Where Technology and Engineering Meet", Springer Science and Business Media LLC, 2018  
Crossref 12 words — < 1%
- 
- 14 [www.scribd.com](http://www.scribd.com)  
Internet 11 words — < 1%
- 
- 15 Advances in FRP Composites in Civil Engineering, 2011.  
Crossref 10 words — < 1%
- 
- 16 Milena Kucharska, Justyna Jaskowska-Lemanska. "Properties of a bond between the steel reinforcement and the new generation concretes – a review", IOP Conference Series: Materials Science and Engineering, 2019 10 words — < 1%

- 
- 17 [www.matec-conferences.org](http://www.matec-conferences.org) 10 words — < 1%  
Internet
- 
- 18 Cristina Vázquez-Herrero, Isabel Martínez-Lage, Gerardo Aguilar, Fernando Martínez-Abella. "Evaluation of strand bond properties along the transfer length of prestressed lightweight concrete members", *Engineering Structures*, 2013 9 words — < 1%  
Crossref
- 
- 19 Danying Gao, Yunchao Huang, Gang Chen, Lin Yang. "Bond stress distribution analysis between steel bar and steel fiber reinforced concrete using midpoint stress interpolation method", *Construction and Building Materials*, 2020 9 words — < 1%  
Crossref
- 
- 20 [issuu.com](http://issuu.com) 9 words — < 1%  
Internet
- 
- 21 Byung Hwan Oh, Se Hoon Kim. "Realistic Models for Local Bond Stress-Slip of Reinforced Concrete under Repeated Loading", *Journal of Structural Engineering*, 2007 8 words — < 1%  
Crossref
- 
- 22 Changhai Zhai, Bing Lu, Weiping Wen, Duofa Ji, Lili Xie. "Experimental study on shear behavior of studs under monotonic and cyclic loadings", *Journal of Constructional Steel Research*, 2018 8 words — < 1%  
Crossref
- 
- 23 Chunyi Xu, Moncef L. Nehdi, Maged A. Youssef, Tao Wang, Lei V. Zhang. "Seismic performance of 8 words — < 1%

RC beam-column edge joints reinforced with austenite stainless steel", Engineering Structures, 2021

Crossref

24 Crescentino Bosco, Francesco Tondolo. "Bond Performance in Machined Reinforcing Bar for Reinforced Concrete", Applied Mechanics and Materials, 2012

8 words — < 1%

Crossref

25 Huai-shuai Shang, Feng-kun Cui, Peng Zhang, Tie-jun Zhao, Guo-sheng Ren. "Bond behavior of steel bar embedded in recycled coarse aggregate concrete under lateral compression load", Construction and Building Materials, 2017

8 words — < 1%

Crossref

26 J.J. Orr, Antony Darby, Tim Ibell, Nick Thoday, Pierfrancesco Valerio. "Anchorage and residual bond characteristics of 7-wire strand", Engineering Structures, 2017

8 words — < 1%

Crossref

27 T. Blesslin Sheeba, A. Albert Raj, D. Ravikumar, S. Sheeba Rani, P. Vijayakumar, Ram Subbiah. "Analysis of silica based prosthetic human teeth using 3D printing machine for dental assistance", Materials Today: Proceedings, 2020

8 words — < 1%

Crossref

28 Wang, H.. "An analytical study of bond strength associated with splitting of concrete cover", Engineering Structures, 200904

8 words — < 1%

Crossref

29 [downloads.hindawi.com](https://downloads.hindawi.com)

Internet

8 words — < 1%

30 [infoscience.epfl.ch](https://infoscience.epfl.ch)

Internet

8 words — < 1%

31 link.springer.com

Internet

8 words — < 1%

32 ntl.bts.gov

Internet

8 words — < 1%

33 spexternal.modot.mo.gov

Internet

8 words — < 1%

34 Fudong Ma, Mingke Deng, Hongkan Fan, Yong Yang, Hongzhe Sun. "Study on the lap-splice behavior of post-yield deformed steel bars in ultra high performance concrete", Construction and Building Materials, 2020

Crossref

6 words — < 1%

35 Prince, M. John Robert, and Bhupinder Singh. "Bond behaviour of normal- and high-strength recycled aggregate concrete", Structural Concrete, 2014.

Crossref

6 words — < 1%

EXCLUDE QUOTES OFF

EXCLUDE MATCHES OFF

EXCLUDE BIBLIOGRAPHY ON